

Enhancing the photo-luminescence stability of $CH_3NH_3PbI_3$ film with ionic liquids

Weifeng Ma(马威峰), Chunjie Ding(丁春杰), Nasrullah Wazir, Xianshuang Wang(王宪双), Denan Kong(孔德男), An Li(李安), Bingsuo Zou(邹炳锁), and Ruibin Liu(刘瑞斌)

Citation: Chin. Phys. B, 2022, 31 (**3**): 037802. DOI: 10.1088/1674-1056/ac3067

Journal homepage: http://cpb.iphy.ac.cn; http://iopscience.iop.org/cpb

What follows is a list of articles you may be interested in

Surface-enhanced fluorescence and application study based on Ag-wheat leaves

Hongwen Cao(曹红文), Liting Guo(郭立婷), Zhen Sun(孙祯), Tifeng Jiao(焦体峰), and Mingli Wang(王明利)

Chin. Phys. B, 2022, 31 (**3**): 037803. DOI: 10.1088/1674-1056/ac1f0d

Combined effects of carrier scattering and Coulomb screening on photoluminescence in InGaN/GaN quantum well structure with high In content

Rui Li(李睿), Ming-Sheng Xu(徐明升), Peng Wang(汪鹏), Cheng-Xin Wang(王成新), Shang-Da Qu(屈尚达), Kai-Ju Shi(时凯居), Ye-Hui Wei(魏烨辉), Xian-Gang Xu(徐现刚), and Zi-Wu Ji(冀子武)

Chin. Phys. B, 2021, 30 (**4**): 047801. DOI: 10.1088/1674-1056/abd692

Thickness-dependent excitonic properties of atomically thin 2H-$MoTe_2$

Jin-Huan Li(李金焕), Dan Bing(邴单), Zhang-Ting Wu(吴章婷), Guo-Qing Wu(吴国庆), Jing Bai(白静), Ru-Xia Du(杜如霞), Zheng-Qing Qi(祁正青)

Chin. Phys. B, 2020, 29 (**1**): 017802. DOI: 10.1088/1674-1056/ab5a3a

Spectral properties of Pr:CNGG crystals grown by micro-pulling-down method

Yan-Yan Xue(薛艳艳), Na Li(李纳), Dong-Hua Hu(胡冬华), Qing-Song Song(宋青松), Xiao-Dong Xu(徐晓东), Dong-Hai Wang(王东海), Qing-Guo Wang(王庆国), Dong-Zhen Li(李东振), Zhan-Shan Wang(王占山), Jun Xu(徐军)

Chin. Phys. B, 2019, 28 (**8**): 087801. DOI: 10.1088/1674-1056/28/8/087801

Influence of annealing treatment on the luminescent properties of Ta:*β*-Ga_2O_3 single crystal

Xiaowei Yu(余小威), Huiayuan Cui(崔慧源), Maodong Zhu(朱茂东), Zhilin Xia(夏志林), Qinglin Sai(赛青林)

Chin. Phys. B, 2019, 28 (**7**): 077801. DOI: 10.1088/1674-1056/28/7/077801

Enhancing the photo-luminescence stability of $CH_3NH_3PbI_3$ film with ionic liquids

Weifeng Ma(马威峰), Chunjie Ding(丁春杰), Nasrullah Wazir, Xianshuang Wang(王宪双), Denan Kong(孔德男), An Li(李安), Bingsuo Zou(邹炳锁), and Ruibin Liu(刘瑞斌)†

Beijing Key Laboratory of Nanophotonics and Ultrafine Optoelectronic Systems, School of Physics, Beijing Institute of Technology, Beijing 100081, *China*

(Received 13 August 2021; revised manuscript received 7 October 2021; accepted manuscript online 18 October 2021)

The methylammonium lead triiodide ($CH_3NH_3PbI_3$)-based perovskite shows a great alluring prospect in areas of solar cells, lasers, photodetectors, and light emitting diodes owing to their excellent optical and electrical advantages. However, it is very sensitive to the surrounding oxygen and moisture, which limits its development seriously. It is urgent to spare no effort to enhance its optical and electrical stability for further application. In this paper, we synthesize the $MAPbI_3$ perovskite film on the glass substrate with/without the ionic liquid (IL) of 1-Butyl-3-methylimidazolium tetrafluoroborate ($BMIMBF_4$) by a simple two-step sequential solution method. The additive of $BMIMBF_4$ can improve the quality of crystal structure. Moreover, the photo-luminescence (PL) intensity of $MAPbI_3$ film with $BMIMBF_4$ is much stronger than the pure $MAPbI_3$ film after a week in the air, which is almost ten-fold of the pure one. Meanwhile, under the illumination of 405-nm continuous wave (CW) laser, the fluorescent duration of the $MAPbI_3$ film with $BMIMBF_4$ is approximately 2.75 min, while the pure $MAPbI_3$ film is only about 6 s. In fact, ionic liquid of $BMIMBF_4$ in the perovskite film plays a role of passivation, which prevents the dissolution of $MAPbI_3$ into CH_3NH_3 and PbI_2 and thus enhances the stability of environment. In addition, the ionic liquid of $BMIMBF_4$ possesses high ionic conductivity, which accelerates the electron transport, so it is beneficial for the perovskite film in the areas of solar cells, photodetectors, and lasers. This interesting experiment provides a promising way to develop the perovskite's further application.

Keywords: $CH_3NH_3PbI_3$ perovskite film, photo-luminescence, $BMIMBF_4$ ionic liquid

PACS: 78.55.–m, 78.68.+m, 78.66.Sq **DOI:** 10.1088/1674-1056/ac3067

1. Introduction

In recent years, hybrid organic–inorganic lead halide perovskites (with general formula ABX_3) and perovskite-type materials have been attracting a large amount of attention, owing to their enormous optical and electrical characters, such as strong absorption, long electron–hole diffusion lengths, and relatively low trap densities.[1–3] Those outstanding characteristics give them promising prospect in fields including the solar cells, lasers, light emitting diodes, and photodetectors.[4–7] Among those excellent materials, the iodide-based cubic perovskite $CH_3NH_3PbI_3$ ($MAPbI_3$) with direct band gap (1.68 eV) shows great application in infrared emission, lasers, photodetectors, and solar cells.[8,9] For example, the power conversion efficiency of $MAPbI_3$ solar cells have been increased to as high as 22.1%.[10,11] Song and the cooperators have demonstrated that the dynamically tuned micro-lasers based on the $MAPbI_3$ perovskite exhibit its process in optical memory, flip–flop, and ultrafast switches.[12] However, $MAPbI_3$ perovskite is very sensitive to the oxygen and moisture,[11,13] which prevents its further development. The $MAPbI_3$ can react with the water and dissolve into CH_3NH_3 and PbI_2, which induces the decrease of absorption intensity across the visible light and a distinct change of the crystal structure.[14,15] More and more researchers give their smart efforts to develop perovskite materials with strong moisture resistance. Lu *et al.* implemented a series of calculations to demonstrate an effective strategy to develop perovskite materials with no or a minor photo-striction effect.[16] In fact, various modifications and engineering aspects have been applied to solve the issue. Among those programs, ionic liquids are considered as an ideal additive to enhance the properties, because ionic liquid, a salt, generally consists of large organic cation and various organic or inorganic anion, making it possess the properties of high ionic conductivity, thermal and electrochemical stability.[17,18] Tang and his cooperators have investigated the ionic liquid of 1-butyl-2,3-dimethylimidazolium chloride ([BMMIm]Cl) in carbon-based cesium lead bromide ($CsPbBr_3$) perovskite solar cells, verifying that it is used as a modification layer for passivating the surface defects and can increase the efficiency to 9.92%.[19] The assistance of thiocyanate in $MAPbI_3$ photodetector has greatly enhanced its stability of electrical properties, the light and dark current could almost keep immovable for 10 days.[18] Here we introduce the ionic liquid of $BMIMBF_4$ into PbI_2 mixture ($MAPbI_3$ precursor solution) when preparing perovskite film. Interestingly, the additive of $BMIMBF_4$ improves the crystalline quality of perovskite film with fewer defects and enhances its stability in the ambient environment.

†Corresponding author. E-mail: liusir@bit.edu.cn

© 2022 Chinese Physical Society and IOP Publishing Ltd

The photoluminescence intensity of the film with $BMIMBF_4$ is about ten-fold of that without $BMIMBF_4$ after one week in the ambient environment. Furthermore, with the 405-nm CW laser focusing on the film, the fluorescent duration of perovskite with $BMIMBF_4$ is as long as 2.75 min, while the film without $BMIMBF_4$ is only 6 s. This interesting result is meaningful in the perovskite's development, which verifies an important method of adding ionic liquid of $BMIMBF_4$ in the precursor solution to improve its stability.

2. Experimental details

2.1. Materials synthesis

All the chemicals including PbI_2 (purity 99.999%, Aladdin), CH_3NH_3I (99.999%, Aladdin), dimethyl sulfoxide (DMSO, 99.9%, Aladdin), isopropanol (> 99.9%, Macklin), and 1-Butyl-3-methylimidazolium tetrafluoroborate ($BMIMBF_4$, 97%, Aladdin) were used without further treatment. The glass substrate was cleaned in the ultrasonic bath by deionized water, ethanol, acetone, isopropanol, and deionized water for 15 min respectively, followed by the ozone treatment in an UV-ozone cleaner for 10 min. First, PbI_2 (0.461 g) was entirely dissolved in the DMSO (1 mL), followed by the ionic liquid of $BMIMBF_4$ (20 μL). A clear yellow solution was achieved after stirring. Second, CH_3NH_3I (0.1 g) was entirely dissolved in the isopropanol (2 mL), which changed to a transparent solution after stirring at 60 °C for 2 h, because it is difficult to dissolve at room temperature. Third, the PbI_2 mixture of 50 μL was dropped on the glass substrate, which is fixed on the spin coater as shown in Fig. 1(a). After it spun at 3000 rpm for 10 s, the CH_3NH_3I solution of 50 μL was dropped and continued to spin for 20 s. At the same time the film was to be black. Then the substrate was put on the hot plate at 150 °C for 30 min, at this moment the $MAPbI_3$ film with ionic liquid, which was named film (II). The film without ionic liquid named after film (I) was synthesized by the same procedure, except that there is no ionic liquid in PbI_2 precursor solution. Figure 1(a) (IV) shows the passivation effect of the $MAPbI_3$ film after adding $BMIMBF_4$. It is worth mentioning that all of the synthesis and fabrication procedures are carried out in the glove box.

2.2. Device fabrication

After the synthesis of film (I) and film (II) on the glass, the silver (Ag) electrodes with a thickness of 300 nm were deposited by the vacuum evaporation system, followed by the silver lines attached to the electrode for extra connection with probes.

2.3. Characteristics

The scanning electron microscopy (SEM) measurements were implemented to measure the morphology (Carl Zeiss, Supra 55). The x-ray diffraction (XRD) measurements were carried out in a Bruker Advance D8 Diffractometer instrument in the 2θ range of 10°–70° with the speed of 1°/min. The absorption and transmission spectrums were taken in the UV-Vis spectrophotometer (UV-6100, purchased from Shanghai). The PL spectra were tested by a μ-PL system with a 405-nm CW laser as the excitation source. A Keithley 4200CS with corresponding mode-locked amplifier is used to measure the *I*–*V* curves and light response.

3. Results and discussion

Figures 1(b) and 1(c) show their optical microscope photographs, which give a larger view and declare the films are uniform and homogeneous. For details, figures 1(d) and 1(e) give the SEM images of film (I) and film (II), respectively. Figure 1(d) shows that the film (I) is homogeneous in micro area, but still has lots of grain boundaries due to the storage process after being prepared. In Fig. 1(e), the SEM image of film (II) exhibits the uniform and smooth surface. Furthermore, the amount of grain boundaries is fewer than that of the film (I), suggesting that the film (II) possesses a better crystallinity and stability. Clearly, the microcrystals of film (II) are similar in size to the film (I). And the additive of $BMIMBF_4$ can really improve the crystallinity structure quality, which has been further confirmed by the XRD spectra.

As shown in Fig. 2(a), the XRD patterns show the typical diffraction peaks (110) and (220), which are located at 13.97° and 28.2°, respectively.[20,21] The positions of those XRD peaks of film (I) and film (II) are all the same, indicating that both of their crystal structures are cubic phase. However, the relative strength of the main diffraction peaks increases largely after the addition of ionic liquid, which implies that the film (II) has better crystallinity. In the XRD pattern of film (I), there is a diffraction peak at 11.1°, which is corresponding to the PbI_2 crystal, illustrating that film (II) has been resolved a little, while there is no diffraction peak at 11.1° in the XRD spectrum of film (II). It declares obviously that the film (II) has not been resolved obviously and is more stable than the film (I). As shown in Fig. 2(b), the emission peaks of the PL spectra of film (I) and film (II) are centered at 758 nm and 761 nm, respectively, which consists with the band gap of $MAPbI_3$.[20] The difference of their PL peaks about 3 nm can be attributed to the ambient environment influence. Furthermore, both of the full width at half maxima (FWHM) are about 35 nm close to the FWHM reported in the perovskite film, indicating that the films are with high quality.[22] The absorption spectra are shown in Fig. 2(c). For film (I), the absorption begins from the wavelength of 760 nm, consisting with the band gap wavelength of $CH_3NH_3PbI_3$ crystal.[4,23,24] While the absorption spectrum of film (II) begins about 770 nm, but the absorp-

tion intensity at wavelength range from 750 nm to 300 nm is smaller than the film (I). It is because that the ionic liquid effectively promotes the growth of crystal grains, reduces the grain boundaries inside the crystal, and makes the surface of the perovskite smooth as a mirror, thereby reducing the absorption of external light.

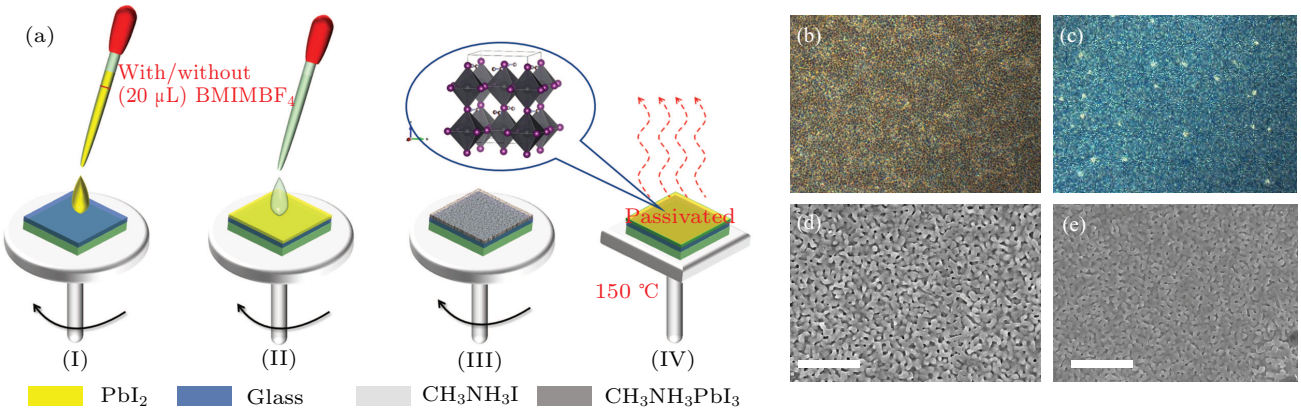


Fig. 1. (a) Schematic diagrams of the synthesis processes. Panels (b) and (c) are the optical images of film (I) and film (II). Panels (d) and (e) are SEM images of film (I) and film (II), respectively. The scale bar is 3 μm.

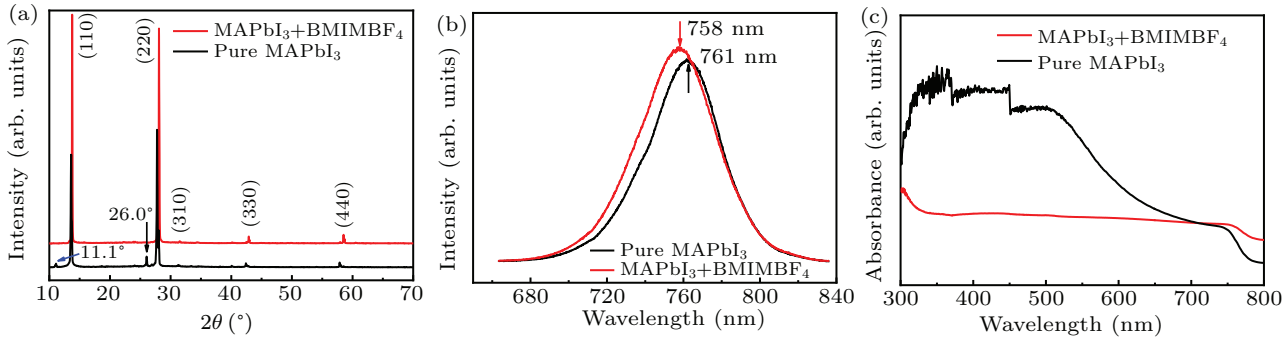


Fig. 2. (a) XRD pattern of film (I) (black line) and film (II) (red line). (b) The PL spectra of film (I) and film (II) measured immediately after they were prepared. (c) Absorbance spectra of film (I) (black line) and film (II) (red line).

To further illustrate the stability, we measure the PL spectrum of film (I) and film (II) after one week. As we can see in Fig. 3(a), the PL peak intensity of film (I) is enormously weaker than before, while the PL peak centered at 763 nm of film (II) (red line) is stronger largely than that of film (I) (black line). What is more, compared to the FWHM of film (II) as prepared in Fig. 2(b), the FWHM after one week becomes wider to 49 nm because of the shallow bound states generated from crystal damage induced by the moisture or oxygen, which also makes the PL peak redshifts to 763 nm of film (II) (red line). Importantly, its intensity is much stronger than that of film (I) (black line), which can be interpreted as ionic liquids provide chemical stability by filling I^- or MA^+ vacancies in the perovskite lattice, and immobilize the migrated ions through ionic interaction, preventing ion migration from the perovskite lattice to achieve passivation.[25]

Meanwhile, as shown in Figs. 3(b) and 3(c), the dark-field optical images emphasize the photo-luminescence intensity difference again clearly. The red light of film (II) (Fig. 3(c)) is very obvious even though it has been kept in the ambient environment for one week, while there is not any signal at all of film (I) (Fig. 3(b)). As shown in Fig. 3(d) (film (I)) and 3(e) (film (II)), the time-dependent PL intensities further demonstrate the duration of the emission process, which are well fitted by one exponential function with time constant of 6 s (as shown in 211790-SI-video_1) for film (I) and 2.75 min (as shown in 211790-SI-video_2) for film (II), respectively. It suggests that the fluorescent duration of film (I) is much shorter than that of film (II) under the illumination of 405-nm CW laser. Under ultraviolet (UV) illumination, the decomposed reaction will speed up due to the stripping of effective samples and structural damages.[26] However, even after one week the film (II) still emits strong red light with high intensity for a long time of 2.75 min, illustrating that the additive of $BMIMBF_4$ improves the stability enormously.

In addition, figure 4(a) shows the *I*–*V* curves. In the dark, under the bias voltage of 2 V, the current of film (I) is about 2.6×10^{-11} A, while the current of film (II) rises to 1.7×10^{-10} A, indicating the resistance decreases from 7.7×10^{10} Ω to 1.17×10^{10} Ω, namely the electron concentration increases enormously. As shown in Fig. 4(b), the normalized light response curves illustrate that their rise time and delay time differ a lot: the rise time of film (II) is about 0.27 s, which is shorter than 0.98 s of film (I), and the delay time of

film (II) is 0.47 s, which is also shorter than 1.06 s of film (I), which is contributed to the better crystallinity than before and high conductivity of $BMIMBF_4$.

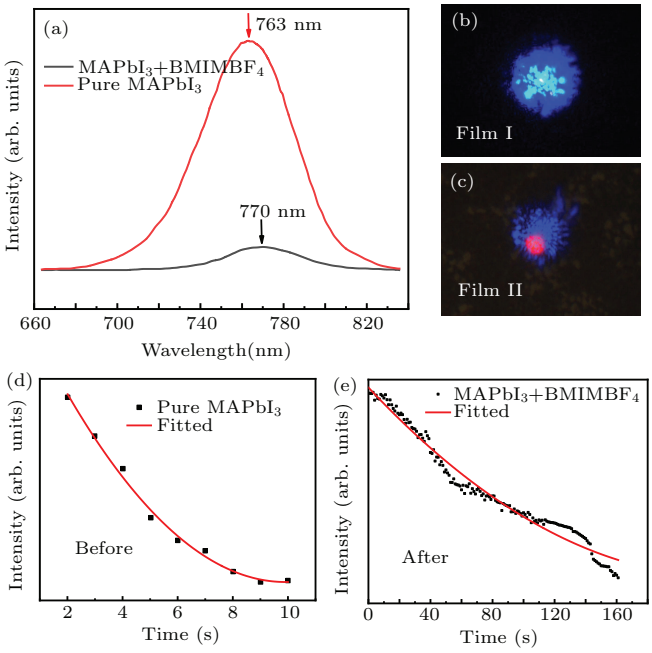


Fig. 3. (a) The PL spectra of film (I) and film (II) measured after one week. The dark-field optical microscope of film (I) [panel (b)] and film (II) [panel (c)] after one week under the focus of 405-nm laser. Panels (d) and (e) are the experimental data (dotted) and the corresponding fitting curves of film (I) and film (II) fluorescent duration, respectively.

As we all know, the ionic liquid consists of large organic cation and various organic or inorganic anion generally, which effectively reduce the inhibition of charge recombination and trapping state through the interaction between the amino lone electron pair of the ionic liquid and the unsaturated Pb^{2+} in the perovskite.[27] Due to the bulky size of the cation or sometimes, of both the cation and anion, the interionic space is very large, hence the attractive electrostatic force becomes weaker. As a result, those are liquid in nature below or around 100 °C.[28] Figure 4(c) shows that the chemical structure of $BMIMBF_4$ molecule where the molecule has two parts, amino group and anion BF_4^-.[29] In the prepared process, the amino group will combine with the $CH_3NH_3^+$ as shown in Fig. 4(d), where the red sphere is corresponding to the amino group. Here the interionic electrostatic force is stronger than that of the volatile organic liquids, which make them almost non-volatile, hence it plays a role of passivation.[29] Another factor of ionic liquid to enhance the electrical properties is that the ionic liquid possesses high ionic conductivity and thermal conductivity, increasing the electron concentration and decreasing the dissolution process, which is important for the electron transport.

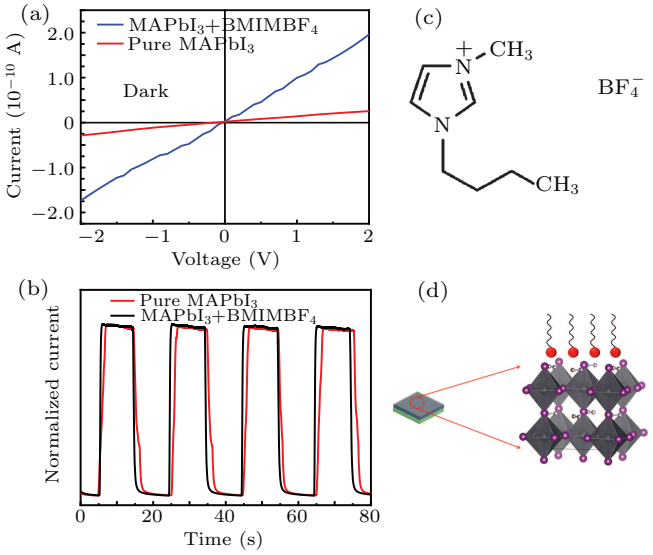


Fig. 4. (a) The *I*–*V* curves of film (I) (red) and film (II) (blue). (b) Normalized light response of film (I) (red) and film (II) (black). (c) Chemical structure of $BMIMBF_4$ molecule. (d) Partial enlarged schematic diagram of the device structure.

Table 1. Comparison of using additive engineering to enhance the stability of $CH_3NH_3PbI_3$.

Type	Device structure	Stability	Ref.
MgI_2	FTO/c-TiO_2/m-TiO_2/PVK/ spiro-OMeTAD/Au	90% of its initial value after 600 h in RH 30%–40% under dark	[31]
DF-C_{60}	ITO/NiO_x/PVK/bis-C60/Ag	Over 83% of initial PCE after 720 h in RH 60%±5% under dark	[32]
Caffeine	FTO/c-TiO_2/PVK/ spiro-OMeTAD/MoO_3/Ag	86% of initial PCE after 1300 h at 85 °C under dark	[33]
Thiourea	FTO/c-TiO_2/m-TiO_2/PVK/ spiro-O Me TAD/Au	85% of initial PCE after 1200 h under dark	[34]
$IMPbI_3$	FTO/c-TiO_2/m-TiO_2/PVK/ spiro-OMeTAD/Au	Over 70% of initial PCE after 1000 h under continuous operation at MPPT	[35]
EATZ	FTO/c-TiO_2/m-TiO_2/PVK/carbon	94% of initial PCE after 840 h in RH 20% under dark	[36]
ETI	FTO/c-TiO_2/m-TiO_2/PVK/spiro-OMeTAD/Au	83% of initial PCE after 700 h at 60 °C under continuous light illumination	[37]
$BMIMBF_4$	Single film	I ten-fold of initial PL intensity after a week in the air, II 27.5 times of initial fluorescent duration under the illumination of 405-nm CW laser	this work

Zhang and his cooperators highlight that the poor chemical stability is intrinsic to $CH_3NH_3PbI_3$ and suggests that element-substitution may solve the chemical stability problem in hybrid halide perovskite solar cells.[30] As shown in Table 1, Lewis acid,[31,32] Lewis base based on the donor type,[33,34] low-dimensional perovskites,[35] and ionic liquid[36,37] are effective to enhance the stability of the $MAPbI_3$ film. The excellent luminescence performance and stability of the $MAPbI_3$ film proves that this method is feasible. In short, all of the excellent results indicate that the additive of $BMIMBF_4$ improves the film's stability and electric performance, providing a promising way to develop the perovskite's further application.

4. Conclusion

In conclusion, we successfully synthesized $MAPbI_3$ films of high crystallinity quality with/without ionic liquid. And it is demonstrated that the additive of ionic liquid $BMIMBF_4$ can improve the crystallinity quality and enhance the stability largely in the ambient environment, thus hindering the perovskite's dissolution. The PL intensity of the film with $BMIMBF_4$ is about ten-fold of that without $BMIMBF_4$ after being stored for a week in the ambient environment. Furthermore, the fluorescent duration of pure perovskite film without $BMIMBF_4$ is about 6 s, while the perovskite film with $BMIMBF_4$ is as long as 2.75 min under the focus of 405-nm CW laser. Here the ionic liquid of $BMIMBF_4$ plays a role of passivation owing to combination with perovskite film and its large organic cation, as a result, it can prevent the reaction with the oxygen or moisture. Meanwhile, according to the *I*–*V* curves, the resistance of film (II) decreases obviously because of ionic liquid's high ionic conductivity and thermal conductivity, which increase the electron concentration and decrease the dissolution process. Therefore, the additive of $BMIMBF_4$ is highly effective for the electron transport on the glass substrate. In a word, the approach is very significant for the stability and electric performance, which gives a bright promising application in perovskite development.

Acknowledgements

Project supported by the National Key Research and Development Program of China (Grant No. 2018YFC2001100), the Natural National Science Foundation of China (Grant No. 61574017), the Fundamental Research Funds for Central Universities, China (Grant No. 2017CX10007), and the Open Foundation of Guangxi Key Laboratory of Processing for Non-ferrous Metals and Featured Materials, Guangxi University (Grant No. 2020GXYSOF08).

References

[1] Xing G, Mathews N, Sun S, Lim S S, Lam Y M, Grätzel M, Mhaisalkar S and Sum T C 2013 *Science* **342** 344
[2] Stranks S D, Eperon G E, Grancini G, Menelaou C, Alcocer M J P, Leijtens T, Herz L M, Petrozza A and Snaith H J 2013 *Science* **342** 341
[3] Michael M, Lee J T, Tsutomu M, Takurou N M and Henry J S 2012 *Science* **338** 643
[4] Tombe S, Adam G, Heilbrunner H, Apaydin D H, Ulbricht C, Sariciftci N S, Arendse C J, Iwuoha E and Scharber M C 2017 *J. Mater. Chem. C* **5** 1714
[5] Fang Y and Huang J 2015 *Adv. Mater.* **27** 2804
[6] Leung S F, Ho K T, Kung P K, Hsiao V K S, Alshareef H N, Wang Z L and He J H 2018 *Adv. Mater.* **30** 1704611
[7] Wei H, Tang Y, Feng B and You H 2017 *Chin. Phys. B* **26** 128801
[8] Li P, Chen Y, Yang T, Wang Z, Lin H, Xu Y, Li L, Mu H, Shivananju B N, Zhang Y, Zhang Q, Pan A, Li S, Tang D, Jia B, Zhang H and Bao Q 2017 *ACS Appl. Mater. Interfaces* **9** 12759
[9] Zhang X, Dong X, Wang S, Liu H, Hu W and Li X 2021 *Chem. Eng. J.* **404** 125957
[10] Saliba M, Matsui T, Seo J Y, Domanski K, Correa-Baena J P, Nazeeruddin M K, Zakeeruddin S M, Tress W, Abate A, Hagfeldt A and Gratzel M 2016 *Energy Environ. Sci.* **9** 1989
[11] You J, Yang Y, Hong Z, Song T B, Meng L, Liu Y, Jiang C, Zhou H, Chang W H, Li G and Yang Y 2014 *Appl. Phys. Lett.* **105** 183902
[12] Zhang N, Fan Y, Wang K, Gu Z, Wang Y, Ge L, Xiao S and Song Q 2019 *Nat. Commun.* **10** 1770
[13] Jia E D, Lou X, Zhou C L, Hao W C and Wang W J 2017 *Chin. Phys. B* **26** 068803
[14] Yang J, D.Siempelkamp B, Liu D and Kelly T L 2015 *ACS Nano* **9** 1955
[15] Jin F, Ji J T, Xie C, Wang Y M, He S N, Zhang Lei, Yang Z R, Yan F and Zhang Q M 2019 *Chin. Phys. B* **28** 076102
[16] Lu Y B, Cong W Y, Guan C, Sun H, Xin Y, Wang K and Song S 2019 *J. Mater. Chem. A* **7** 27469
[17] Wan Y, Dong S, Wang Y, Yang L, Qin W, Cao H, Yao C, Ge Z and Yin S 2016 *RSC Adv.* **6** 97848
[18] Chu Y, Chen Y, Zhou J, Zhou B and Huang J 2019 *ACS Appl. Mater. Interfaces* **11** 14510
[19] Zhang W, Liu X, He B, Gong Z, Zhu J, Ding Y, Chen H and Tang Q 2020 *ACS Appl. Mater. Interfaces* **12** 4540
[20] Marand Z R, Kermanpur A, Karimzadeh F, Barea E M, Hassanabadi E, Anaraki E H, Julian-Lopez B, Masi S and Mora-Sero I 2020 *Nanomaterials* **10** 872
[21] Fan P, Gu D, Liang G X, Luo J T, Chen J L, Zheng Z H and Zhang D P 2016 *Sci. Rep.* **6** 29910
[22] Chen L C, Chen J C, Chen C C and Wu C G 2015 *Nanoscale Res. Lett.* **10** 312
[23] Wu Z Y, Jian B L and Hsu H C 2019 *Opt. Mater. Express* **9** 1882
[24] Schouwink P, Ley M B, Tissot A, Hagemann H, Jensen T R, Smrcok L and Cerny R 2014 *Nat. Commun.* **5** 5706
[25] Chu W, Yang J, Jiang Q, Li X and Xin J 2018 *Appl. Surf. Sci.* **440** 1116
[26] Wang X, Wan S, He Y, Qiu S, Ma X, Wazir N, Tian Y and Liu R 2021 *Spectrochimica Acta Part B: Atomic Spectroscopy* **178** 106123
[27] O'regan B C, Barnes P R F, Li X, Law C, Palomares E and Marin-Beloqui J M 2015 *J. Am. Chem. Soc.* **137** 5087
[28] Ali N, Liang C, Ji C, Zhang H, Sun M, Li D, You F and He Z 2020 *Org. Electron.* **84** 105805
[29] Ji D, Kang Y S and Kang S W 2015 *Sci. Rep.* **5** 16362
[30] Zhang Y Y, Chen S Y, Xu P, Xiang H J, Gong X G, Aron Walsh and Wei S H 2018 *Chin. Phys. Lett.* **35** 036104
[31] Yang F, Kamarudin M A, Kapil G, Hirotani D, Zhang P, Ng C H, Ma T and Hayase S 2018 *ACS Appl. Mater. Interfaces* **10** 24543
[32] Liu X, Lin F, Chueh C C, Chen Q, Zhao T, Liang P W, Zhu Z, Sun Y and Jen A K Y 2016 *Nano Energy* **30** 417
[33] Wang R, Xue J, Meng L, Lee J W, Zhao Z, Sun P, Cai L, Huang T, Wang Z, Wang Z K, Duan Y, Yang J L, Tan S, Yuan Y, Huang Y and Yang Y 2019 *Joule* **3** 1464
[34] Fei C, Li B, Zhang R, Fu H, Tian J and Cao G 2017 *Adv. Energy Mater.* **7** 1602017
[35] Zhang Y, Grancini G, Fei Z, Shirzadi E, Liu X, Oveisi E, Tirani F F, Scopelliti R, Feng Y, Nazeeruddin M K and Dyson P J 2019 *Nano Energy* **58** 105
[36] Wang S, Li Z, Zhang Y, Liu X, Han J, Li X, Liu Z, Liu S and Choy W C H 2019 *Adv. Funct. Mater.* **29** 1900417
[37] Moore D T, Tan K W, Sai H, Barteau K P, Wiesner U and Estroff L A 2015 *Chem. Mater.* **27** 3197